Appl Phys A (2011) 102: 99–103
DOI 10.1007/s00339-010-6022-4

Applied Physics A
Materials Science & Processing

Perfect metamaterial absorber based on a split-ring-cross resonator

Yongzhi Cheng · Helin Yang · Zhengze Cheng · Nan Wu

Received: 7 April 2010 / Accepted: 18 August 2010 / Published online: 9 September 2010

Abstract In this paper, we present a polarization-insensitive metamaterial (MM) absorber which is composed of the dielectric substrate sandwiched with split-ring-cross resonator (SRCR) and continuous metal film. The MM absorber is not limited by the quarter-wavelength thickness and can achieve near-unity absorbance by properly assembling the sandwiched structure. Microwave experiments demonstrate the maximum absorptivity to be about 99% around 10.91 GHz for incident wave with different polarizations. The surface currents distributions of the resonance structure are discussed to look into the resonance mechanism. Importantly, our absorber is only 0.4 mm thick, and numerical simulations confirm that the MM absorber could achieve very high absorptivity at wide angles of incidence for both transverse electric (TE) wave and transverse magnetic (TM) wave. The sandwiched structure is also suitable for designing of a THz and even higher frequency MM absorber, and simulations demonstrate the absorption of 99% at 1.105 THz.

Y. Cheng (✉) · H. Yang
College of Physical Science and Technology, Huazhong Normal University, Wuhan 430079, P.R. China
e-mail: cyz0715@126.com

H. Yang
e-mail: emyang@mail.ccnu.edu.cn

Z. Cheng
The School of Electronic and Information Engineering, XianNing University, Xianning 437100, P.R. China
e-mail: czz8986my@163.com

N. Wu
National Key Laboratory of EMC, China Ship Development and Design Center, Wuhan, 430064, P.R. China
e-mail: nanlife1979@yahoo.com.cn

1 Introduction

Since the hypothesis of simultaneously negative permittivity (ε) and permeability (μ) of media was proposed by Veselago [1] and first microwave experiments were demonstrated by Smith et al. [2], a new class of artificial materials, so-called metamaterials (MMs) has attracted considerable great interest. The research of negative refractive index (NRI) or double-negative material, which usually is composed of sub-wavelength metallic resonance elements [3, 4], has ushered in a new field of science in recent years. The sub-wavelength unit cell that comprises highly conductive and shaped metals such as gold or copper is periodically arranged in the MMs, and, therefore, treated as homogeneous medium. According to effective medium theory, MMs can be characterized by a complex electric permittivity $\tilde{\varepsilon}(\omega) = \varepsilon_1 + i\varepsilon_2$ and magnetic permeability $\tilde{\mu}(\omega) = \mu_1 + i\mu_2$ [5]. MMs have been demonstrated in every technologically relevant spectral range from microwave to optical [6–9]. Generally, more or less power losses could be existence when electromagnetic (EM) waves impinge on MMs. Some applications of MMs are required to minimize losses over the operating frequency range, and the existence of losses could deteriorate the performance of some devices, such as superlenses [10–12]. On the contrary, many applications would be desirable to maximize the metamaterial losses, such as the MM absorber.

N. Engheta first proposed the theoretic view of using metamaterial achieving perfect absorption for EM waves [13], and microwave experiments were first demonstrated by Landy et al. [14], which has become an important aspect in the research of MMs. Recently, from microwave to visible frequencies ranges, various MM absorbers which consist of two or more layers coupling sandwiched resonance structures have been reported [15–20]. The electric response can be obtained from the excitation of the electric resonators by

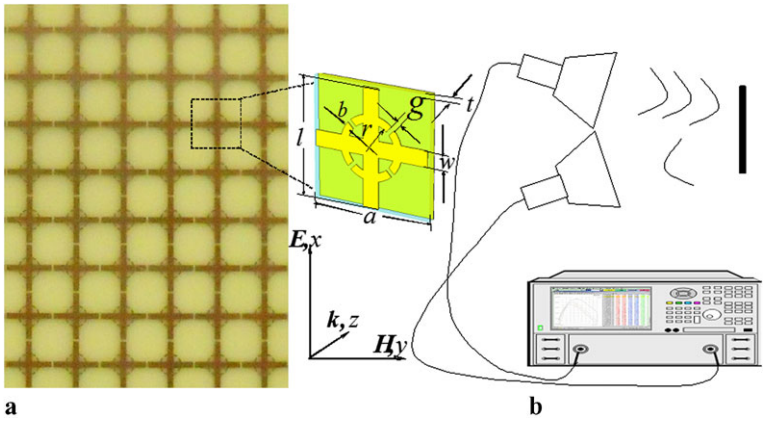

Fig. 1 (**a**) Photograph of a portion of the fabricated MM absorber; (**b**) the schematics of the reflection measurement; the *middle inset* is the unit cell with axis indicating propagation direction of a TEM wave

the electric field, and the magnetic response is provided by the antiparallel currents on the two sides of the substrate. Therefore, it is ideal for resonant absorbers with MMs.

The expression of the absorptivity is $A(\omega) = 1 - R(\omega) - T(\omega)$, where $A(\omega)$, $R(\omega)$, and $T(\omega)$ are the absorptivity, the reflectance, and the transmission as functions of frequency ω respectively. One is required to minimize $R(\omega)$ and $T(\omega)$ simultaneously for making the absorptivity $A(\omega)$ as close to unity as possible. The frequency-dependent transmission $T(\omega)$ and reflectance $R(\omega)$ are mainly determined to be dependent on the complex index of refraction $\tilde{n}(\omega) = \sqrt{\tilde{\varepsilon}(\omega)\tilde{\mu}(\omega)} = n_1 + in_2$ and impedance $\tilde{z}(\omega) = \sqrt{\tilde{\mu}(\omega)/\tilde{\varepsilon}(\omega)} = z_1 + iz_2$ [14]. The absorptivity usually arises from losses within the coupling of electric resonator and dielectric slab. It is possible to absorb both the incident electric and magnetic field tremendously by properly tuning $\tilde{\varepsilon}(\omega)$ and $\tilde{\mu}(\omega)$ and achieving a perfect impedance, matched ($\tilde{z}(\omega) = \sqrt{\tilde{\mu}(\omega)/\tilde{\varepsilon}(\omega)} = 1$) to free space. Comparing the conventional absorber, the MM absorber is not limited by the quarter-wavelength thickness and could achieve near-unity absorbance. Therefore, such MM resonant absorbers could be widely used in thermal imaging, thermal bolometers, wavelength-selective radiators, stealth technology and nondestructive detection [18, 19].

In this paper, a SRCR structure is proposed which combines the dielectric substrate and the continuous metal film to form a perfect MM absorber. For this sandwiched structure, if the resonance and the damping frequencies of the MM sheets are chosen in a proper way, this could allow maintaining sufficiently high field amplitudes at the interfaces, absorbing most of the impinging EM waves' power. To make the absorptivity near unity, exotic metal electric structures and dielectric substrates should be selected and assembled properly. The MM absorber is only 0.4 mm and microwave experiments demonstrate an absorptivity of 99% around 10.91 GHz for an incident wave with different polarizations. The numerical simulations also demonstrate that the MM absorber could be operated well at wide angles of incidence. The simulated absorptivity of 99% at 1.105 THz is also demonstrated by reducing the dimensions (the thickness of the MM absorber is only 6 μm) and dielectric substrate of the MMs elements.

2 Unit cell design, numerical simulation and experiment

The optimized unit cell is presented in the middle inset of Fig. 1. The unit cell of our design composed of an electric SRCR (similar to the LC resonator structure) [21] in the front side, which is primarily responsible for determining $\tilde{\varepsilon}(\omega)$, while the back continuous metal film is designed so that the incident magnetic field drives circulating currents between the two layers. The standard optical lithography processes are used to fabricate the MM absorber sample. The SRCR structure and continuous copper film are etched on the two sides of the FR-4 (lossy) substrate, respectively. The single-layer MM absorber sample is an array of pixels of 15 cm × 15 cm as shown in Fig. 1(a). The dimensions and EM parameters of the sample are the same as that used in simulations. This electric resonant structure has four-fold rotational symmetry with polarization-insensitivity for incident EM wave. The metal elements in both sides are etched as a 20 μm thick copper film with a frequency-independent conductivity $\sigma = 5.8 \times 10^7$ S/m. We use FR-4 (lossy) substrate as the dielectric spacer with a frequency-independent permittivity of $\varepsilon = 5.7 + i0.025$. The unit cell structure is optimized (see inset of Fig. 1) and the geometric parameters are as follows, in millimeters: $a = 6$, $l = 5.8$, $w = 0.8$, $t = 0.4$, $b = 0.4$, $g = 0.2$, $r = 1.2$.

To demonstrate the microwave absorption of our design, a full wave electromagnetic simulation has been performed based on the standard finite-difference time domain (FDTD) method by CST Microwave Studio software. For a TEM plane wave normal incidence, there is no transmission to be examined, as it is blocked off by the continuous metal film [15]. Thus, only the reflectance needs to

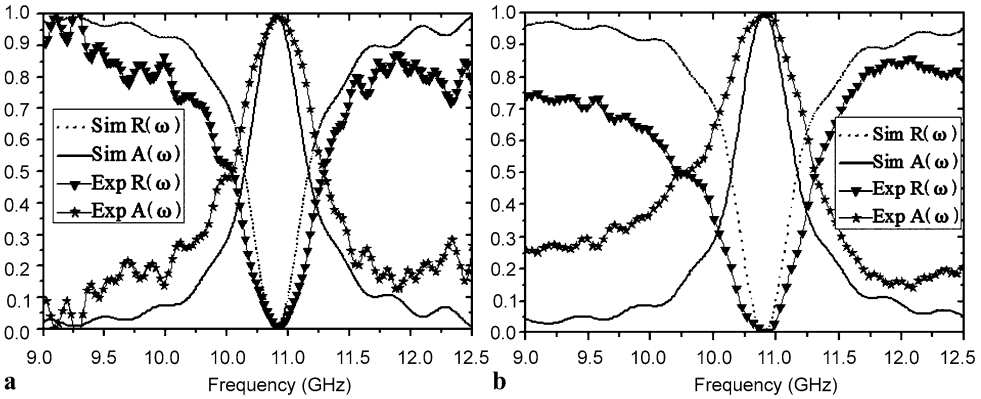

Fig. 2 Simulated and measured EM waves reflection and absorption for two different polarizations (**a**) electric field along the x axis, (**b**) EM polarization rotated 45° along x axis in the $x-y$ plane

be examined in our simulations and experiments. This produces the complex frequency-dependent S parameter: S_{11} is corresponding to the reflection coefficient ($R(\omega) = |S_{11}|^2$), thus the absorptivity is calculated by the equation $A(\omega) = 1 - R(\omega) = 1 - |S_{11}|^2$. By tuning ω_0 of the $\tilde{\varepsilon}(\omega)$ and $\tilde{\mu}(\omega)$ properly, we could achieve $\tilde{\varepsilon}(\omega) = \tilde{\mu}(\omega)$ and thus an impedance matched to free space [18]. The absorptivity may achieve unity ($A(\omega) \to 1$) when the reflection is close to zero ($R(\omega) \to 0$).

To conform the simulations, the experiments were carried out in the free space. The schematics of the reflection measurement is shown in Fig. 1(b). Agilent PNA E8362 vector network analyzer connected to the two standard gain horn antennas was used to measure the reflection properties of a single-layer MM absorber sample. Incident waves with different polarizations could be generated by rotating the horn antennas with the horizontal z axis. For the reflection measurements, the source and receiving horns are on the same side of the sample. The source and receiver horns are each inclined with an angle of about 7.5° with respect to the normal on the sample surface because of experimental limitations. Before measuring the MM absorber sample, the reflection should be calibrated with a perfect conducting metal plate.

3 Results discussion

Simulation and experimental results for different polarizations are displayed in Figs. 2(a) and 2(b) respectively. The simulated reflectance matches reasonably well near the resonance point and there exist slight deviations at lower and higher frequencies. For electric field along the x axis, the reflectance of simulation and experiment are both close to zero around 10.91 GHz; therefore, the corresponding absorptivities are greater than 99% (see Fig. 2(a)). It should be noticed that our structure is highly symmetrical, thus, we could conjecture that it is polarization insensitive for normal incident EM waves. It means that the absorptivity of the MM absorber would be nearly unchanged with different polarizations. To verify this conjecture, we just need to rotate 45° for polarization because of the four-fold rotational symmetry of the resonance structure. In Fig. 2(b), we can clearly see that the absorptivity of simulation and experiment are nearly identical for EM polarization rotating 45° along the x axis in the $x-y$ plane. Obviously, we may believe that the results will be the same for the normal incident wave with any polarization.

Comparing the simulations with the experiments, the simulated results around the resonance frequency point match very well with the measured values. However, there are some discrepancies in the off-resonant area, especially in the lower- and higher-frequency ranges. Several mechanisms may account for this discrepancy. I conjecture that it is mainly due to the tolerances in the fabrication and the imperfection in measurements.

From the simulations and experiments of our designed MM absorber for different polarizations, the absorptivities are both greater than 99%. It reveals that the electric and magnetic are strongly in resonance around 10.91 GHz, $\tilde{\varepsilon}(\omega) = \tilde{\mu}(\omega)$ and near-perfect impedance-matched to the free space, resulting in near-zero reflection. To better understand the physical mechanism of the high absorption, antiparallel current distributions in the two sides of the MM absorber have been examined at the resonance frequency point of 10.91 GHz (Fig. 3). For EM wave normal incidence, the surface current density in the metal SRCR is symmetrical, which is similar to the electric LC resonator [21]. We clearly see that currents in the borderlines and gaps of the SRCR here are stronger than the in-plane case, producing a strong charge accumulation along the $\boldsymbol{E}$ direction, resulting in a strong electric resonance. At the same time, we could imagine that when the incidence wave arrives from the SRCR side, the coupling between the metal SRCR and the continuous metal film will attenuate the power of the wave to a very low value [22]. Thus, we may conclude that the high absorptivity of the MM absorber is mainly due to the local EM resonance. On the other hand, the dielectric substrate also plays an important role in the wave impedance

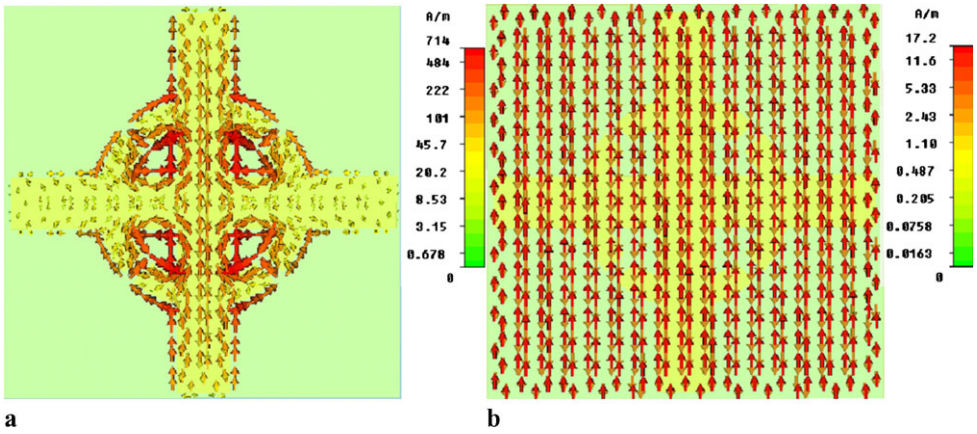

Fig. 3 Simulation results (**a**) and (**b**) the antiparallel current distribution in the two sides driven by magnetic coupling in resonance frequency

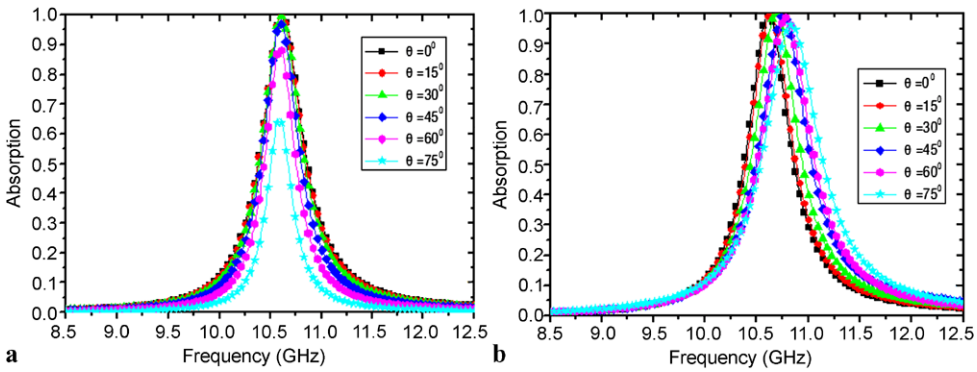

Fig. 4 Simulated absorption at different oblique incident angles (θ) for (**a**) TE and (**b**) TM modes

match. The MM absorber could achieve a near-perfect impedance match ($\tilde{z}(\omega) \approx 1$) when tuning the thickness of the dielectric substrate.

In the above section, we obtained the results under normal incidence for different polarizations. In practical use, EM waves are usually incident onto absorbers with an oblique incidence angle. Therefore, it is necessary to investigate EM absorption of the MM absorber at different oblique incident angles. Figure 4 shows the simulated absorption of our MM absorber at various angles of oblique incidence for TE and TM modes. For the TE case (Fig. 4(a)), it could be found that the absorption peak monotonously decreases with increasing angle of incidence, but still remains higher than 85% for an incident angle (θ) smaller than 60°. Beyond 60°, there is a sudden decrease in the absorptivity. It is mainly due to the incident magnetic flux between the sandwiched structure, becoming less and less with the increase of incidence angle [15]. For the case of TM modes shown in Fig. 4(b), the center frequency of the absorption peak has a slight shift with the increase of incidence angle. However, the absorption peak remains more than 98% for different incident angles. It means that the magnetic flux between the SRCR and copper film is nearly unchanged, and it could provide strong magnetic resonance at all angles of incidence, which is important to maintain impedance match [17]. Simulated results indicate that the MM absorber could work well for oblique incident EM waves over a very large range of incident angles.

From the above discussion, one concludes that our sandwiched structure MM absorber could achieve perfect absorption characteristics. In fact, if the dimensions of the SRCR structure are reduced to micro-, nano- and even lower scale, this will give perfect absorptivity at THz, infrared frequencies and even optical frequencies. What is more, if the SRCR structure is designed to MM absorber for higher frequencies, the fabrication is even more complex. Here, we give an example of a THz MM absorber. Similar to the design of Tao et al. [18], we use polyimide (lossy) with a frequency-independent permittivity of $\varepsilon = 3.5 + i0.003$ as a dielectric spacer. The geometric parameters of the single unit cell are as follows in micrometers: $a = 40$, $l = 38$, $w = 2$, $t = 6$, $b = 0.4$, $g = 0.5$, $r = 16$. The simulation results are presented in Fig. 5, the reflection is near zero and the corresponding absorptivity is higher than 99% at 1.105 THz. Therefore, the SRCR is suitable for designing a THz MM absorber as well. According to the TL model, the LC resonance of SRCR strongly affects the absorption characteristics of the absorber. What is more, the interlayer coupling and other resonances from the adjacent SRCR are also not negligible [23].

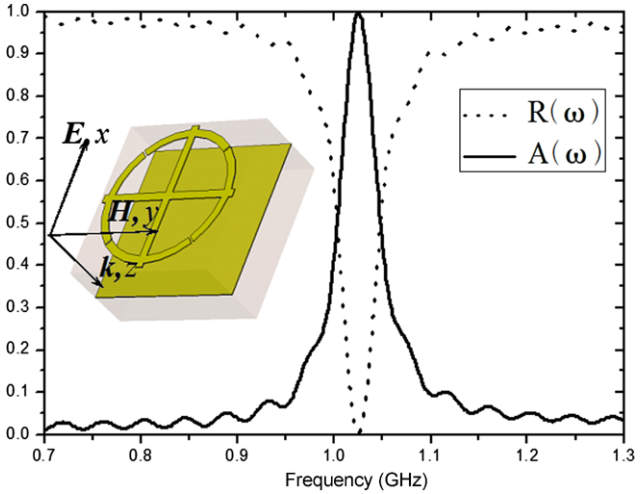

Fig. 5 The simulated reflection (*dash line*) and absorption (*solid line*) curve of the THz MM absorber; the *inset* shows the single unit cell with axis indicating propagation direction

4 Conclusion

In conclusion, we present a sandwiched structure of a MM absorber composed of metal SRCR, dielectric substrate, and continuous metal film. The microwave experiments demonstrate that the absorptivity of the MM absorber could achieve 99% around 10.91 GHz for incident waves with different polarizations, and the numerical simulations demonstrate that it could be operated well at wide angles of incidence. This structure also could be designed as a THz MM absorber, and simulation shows an absorptivity of 99.78% at 1.105 THz. Compared to previous designs [15–18], our device is thinner (only 0.4 mm) and has higher absorptivity (more than 99% in experiment) at gigahertz frequencies range. Our design is narrow-band absorptive and polarization-insensitive for incident EM wave. It is available for some spectrally selective applications, such as in the detection of explosives and wavelength-selective radiators. As previously mentioned, the resonant absorber is not limited by the quarter-wavelength thickness and very thin (about 1/75 of the operation wavelength). Therefore, this may be ideal for certain applications, such as thermal detection and bolometers, due to its perfect absorption for arbitrarily polarized or incoherent light.

Acknowledgements This work was supported by the Science and Technology Research project of Hubei provincial Department of Education under Grant No. D20108202.

References

1. V.G. Veselago, Sov. Phys. Usp. **10**, 509 (1968)
2. D.R. Smith, W.J. Padilla, D.C. Vier, S.C. Nemat-Nasser, S. Schultz, Phys. Rev. Lett. **84**, 4184 (2000)
3. R.A. Shelby, D.R. Smith, S. Schultz, Science **292**, 77 (2001)
4. J.F. Zhou, L. Zhang, G. Tuttle, T. Koschny, C.M. Soukoulis, Phys. Rev. B **73**, 041101(R) (2006)
5. D.R. Smith, J.B. Pendry, J. Opt. Soc. Am. B **23**, 391 (2006)
6. Y. Svirko, N. Zheludev, M. Osipov, Appl. Phys. Lett. **78**, 498 (2001)
7. W.J. Padilla, M.T. Aronsson, C. Highstrete, M. Lee, A.J. Taylor, R.D. Averitt, Phys. Rev. B **75**, 041102R (2007)
8. E. Plum, V.A. Fedotov, A.S. Schwanecke, N.I. Zheludev, Y. Chen, Appl. Phys. Lett. **90**, 223113 (2007)
9. J.F. Zhou, T. Koschny, M. Kafesaki, C.M. Soukoulis, Phys. Rev. B **80**, 035109 (2009)
10. J.B. Pendry, Phys. Rev. Lett. **85**, 3966 (2000)
11. M.W. Feise, P.J. Bevelacqua, J.B. Schneider, Phys. Rev. B **66**, 035113 (2002)
12. A. Fang, T. Koschny, C.M. Soukoulis, Phys. Rev. B **79**, 245127 (2009)
13. N. Engheta, in IEEE Anten and Propagat. Soc. Int. Symp., vol. 2, p. 92 (2002)
14. N.I. Landy, S. Sajuyigbe, J.J. Mock, D.R. Smith, W.J. Padilla, Phys. Rev. Lett. **100**, 207402 (2008)
15. W.R. Zhu, X.P. Zhao, J. Opt. Soc. Am. B **26**, 2382 (2009)
16. Y.Z. Cheng, H.L. Yang, J. Appl. Phys. **108**, 034906 (2010)
17. W.R. Zhu, X.P. Zhao, B. Shi, Y.P. Zhang, Chin. Phys. Lett. **27**, 014204 (2010)
18. H. Tao, C.M. Bingham, A.C. Strikwerda, D. Pilon, D. Shrekenhamer, N.I. Landy, K. Fan, X. Zhang, J. Padilla, R.D. Averitt, Phys. Rev. B **78**, 241103 (2008)
19. N.I. Landy, C.M. Bingham, T. Tyler, N. Jokerst, D.R. Smith, W.J. Padilla, Phys. Rev. B **79**, 125104R (2009)
20. C.G. Hu, Z.Y. Zhao, X.N. Chen, X.G. Luo, Opt. Express **17**, 11039 (2009)
21. D. Schurig, J.J. Mock, D.R. Smith, Appl. Phys. Lett. **88**, 041109 (2006)
22. D.R. Smith, D.C. Vier, T. Koschny, C.M. Soukoulis, Phys. Rev. E **71**, 036617 (2005)
23. Q.Y. Wen, Y.S. Xie, H.W. Zhang, Q.H. Yang, Y.X. Li, Y.L. Liu, Opt. Express **22**, 20256 (2009)